Intermetallics 18 (2010) 2404–2411

Contents lists available at ScienceDirect

Intermetallics

journal homepage: www.elsevier.com/locate/intermet

Determination of the solubility range and crystal structure of the Mg-rich ternary compound in the Ca–Mg–Zn system

Yi-Nan Zhang [a], Dmytro Kevorkov [a], Jian Li [b], Elhachmi Essadiqi [b], Mamoun Medraj [a,*]

[a] Department of Mechanical Engineering, Concordia University, 1455 de Maisonneuve Blvd. W., Montreal, Quebec, Canada H3G 1M8
[b] Materials Technology Laboratory, CANMET, 568 Booth Street, Ottawa, Ontario K1A 0G1, Canada

ARTICLE INFO

Article history:
Received 13 July 2010
Received in revised form
30 July 2010
Accepted 16 August 2010
Available online 25 September 2010

Keywords:
A. Ternary alloy systems
B. Phase diagrams
B. Phase identification
F. Diffraction
F. Electron microprobe

ABSTRACT

The homogeneity range and crystal structure of the Mg-rich ternary solid solution has been determined using SEM, EPMA/WDS, TEM and X-ray diffraction. This compound has the $Ca_3Mg_xZn_{15-x}$ ($4.6 \leq x \leq 12$) formula at 335 °C. The refinement of the XRD patterns was carried out by Rietveld analysis, XRD data has shown that this solid solution crystallizes in hexagonal structure having *P63/mmc* (194) space group and $Sc_3Ni_{11}Si_4$ prototype. The lattice parameters decrease linearly with decreasing Mg content obeying Vegard's law. The fractional atomic occupancy of 6h, 4f, 2b and 12k sites of this compound are function of Mg concentration. Focused Ion Beam has been used to lift TEM specimen of the ternary compound and the hexagonal structure has been confirmed by means of selected area electron diffraction data. Based on the atomic occupancy results and the crystallographic details, a three sublattice (Ca)(Zn)(Mg, Zn)$_4$ model is proposed for this compound.

1. Introduction

Mg-based alloys have attracted much attention as the lightest structural alloys for the aerospace and automotive applications. Ca content in Mg alloys improves strength, castability, and creep and corrosion resistance [1,2]. The addition of Zn to the binary Mg–Ca alloys reinforces the age hardening response [3]. Recently, Zberg et al. [4,5] showed that above a certain percentage of Zn in the system (approximately 28 at.% of Zn), biocompatible metallic glass exists. This metallic glass shows a great potential for the development of biodegradable implants [4,5]. Since the Ca–Mg–Zn system is promising as a next-generation material in both transportation and biomedical applications, having an accurate understanding of the equilibrium in this system is needed.

Many researchers studied the solubility range and the crystal structure of the $Ca_2Mg_6Zn_3$ compound, but their results are contradictory [6–13]. Based on the thermal analysis and metallography, Paris [6] reported a ternary compound with the composition $Ca_2Mg_5Zn_5$, as shown in Fig. 1, but he did not provide any crystallographic information for it. The isothermal section in the Mg–Zn side of the Ca–Mg–Zn system at 335 °C was studied by Clark [7] using metallography and powder X-ray diffraction. He reported two solid solutions β and ω as shown in Fig. 1. These are different from the $Ca_2Mg_5Zn_5$ composition reported by Paris [6]. The compositions of the two ternary compounds and the XRD patterns were mentioned by Clark later in the Joint Committee on Powder Diffraction Standards (JCPDS) [8,9] as $Ca_2Mg_6Zn_3$ and $Ca_2Mg_5Zn_{13}$. The composition of $Ca_2Mg_6Zn_3$ is slightly different from his previous result [7] of β with extensive solubility range, but the composition of $Ca_2Mg_5Zn_{13}$ is consistent with ω. Then, Larinova et al. [10] worked on this system using XRD and reported a ternary compound with $Ca_2Mg_6Zn_3$ composition. Clark [8] and Larinova et al. [10] mentioned that this compound has a hexagonal structure with lattice parameters $a = 9.725$ Å, $c = 10.148$ Å, but did not report the space group and structure type. More recently, Jardim et al. [11,12] and Oh-ishi et al. [13] studied the system by TEM. Both of them reported a ternary compound with $Ca_2Mg_6Zn_3$ composition, which is similar to the compound given in the JCPDS card reported by Clark [8]. However, they reported this compound as a trigonal structure with space group $P\bar{3}1c$, lattice parameters $a = 9.7$ Å, $c = 10$ Å, and $Si_2Te_6Mn_3$ prototype, which does not agree with the hexagonal structure reported by Clark [8] and Larinova et al. [10]. In order to resolve these controversies, the solubility range and crystal structure of this compound are investigated here.

2. Experimental investigation

In order to study the Ca–Mg–Zn ternary system, nine diffusion couples and 36 key alloys were prepared to map the whole isothermal section at 335 °C based on the preliminary thermodynamic model of

* Corresponding author. Tel.: +1 514 585 2424; fax: +1 514 848 3175.
E-mail address: mmedraj@encs.concordia.ca (M. Medraj).
URL: http://users.encs.concordia.ca/%7emmedraj/

0966-9795/$ – see front matter © 2010 Elsevier Ltd. All rights reserved.
doi:10.1016/j.intermet.2010.08.033

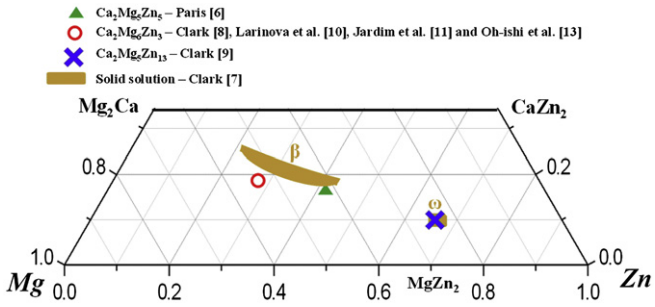

Fig. 1. Ternary solid phases in the Ca–Mg–Zn system.

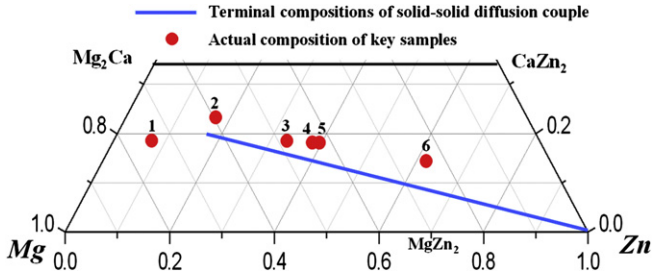

Fig. 2. The composition of the samples and diffusion couple used to determine the solubility range and crystal structure of the Mg-rich ternary compound.

Wasiur–Rahman and Medraj [14]. The details of the experimental determination of this isothermal section will be published soon. Part of this work was directed towards determining the solubility range and the crystal structure of the Mg-rich ternary compound using one diffusion couple and 6 key samples, as illustrated in Fig. 2. The starting materials are high-purity Mg ingot of 99.8%, Zn with purity of 99.99%, and Ca with 99%, all supplied by Alfa Aesar. The key alloys were prepared in an arc-melting furnace with water-cooled copper crucible under a protective argon atmosphere. Samples were re-melted five times to ensure homogeneity. The diffusion couples and key alloys were annealed at 335 °C for 4 weeks.

The homogeneity range of this compound was determined using Electron Probe Microanalysis (EPMA) with Wavelength Dispersive X-Ray Spectrometry (WDS). The error of the EPMA measurements was estimated to be about ±2 at.%. This value was

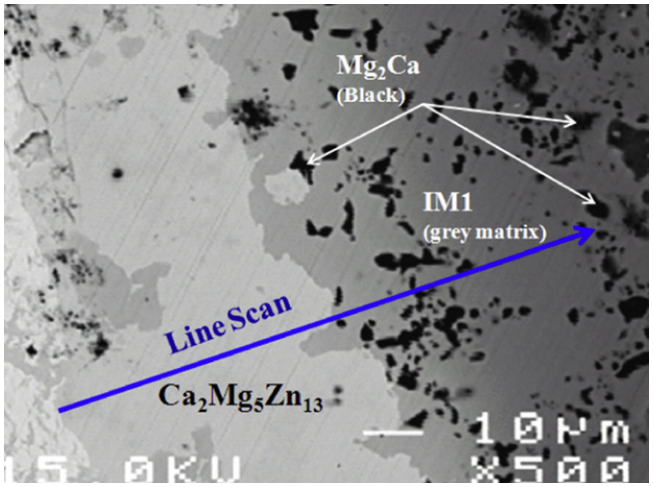

Fig. 3. BE images of $Ca_{20.2}Mg_{63.1}Zn_{16.7}$-Zn solid–solid diffusion couple annealed at 335 °C. for 4 weeks with increased magnification of the area of interest.

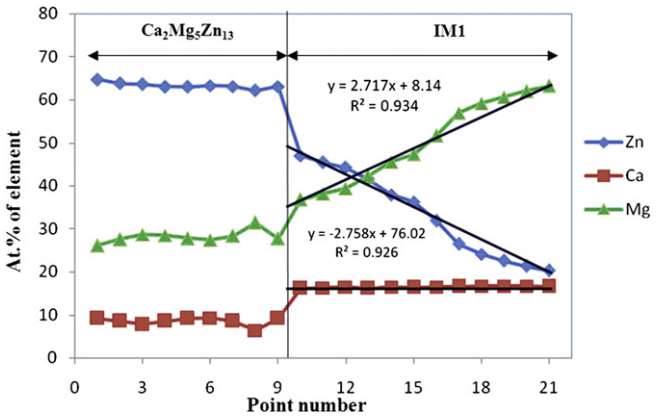

Fig. 4. Composition profiles of the line scan shown in Fig. 3(b).

obtained from the statistical analysis of the compositions of selected phases from several samples. The actual global compositions of the samples were identified by Inductively Coupled Plasma-Mass Spectrometry (ICP-MS). The XRD patterns were obtained using PANanalytical Xpert Pro powder X-ray diffractometer with a CuKα radiation. The XRD spectrum is acquired from 20 to 120° 2θ with a 0.02° step size. X-ray diffraction study of the samples is carried out using X'Pert HighScore Plus Rietveld analysis software and the crystal structure details of the $Sc_3Ni_{11}Si_4$ prototype [15]. Focused Ion Beam (FIB) is used to lift a specimen of the ternary compound from key sample 4 ($Ca_{18.0}Mg_{44.2}Zn_{37.8}$) and to obtain the crystallographic information using TEM. The Selected Area Electron Diffraction (SAED) and CM20 FEG TEM operated at 200 kV are used to analyze this ternary compound.

3. Results and discussion

3.1. Diffusion couple analysis

Backscattered electron images of the solid–solid $Ca_{20.2}Mg_{63.1}Zn_{16.7}$-Zn diffusion couple annealed at 335 °C for 4 weeks are shown in Fig. 3 with increased magnification of the area of interest. During this long-term heat treatment, extensive interdiffusion among Ca, Mg and Zn took place allowing various equilibrium phases to form. The composition of the compound of interest has been determined by EPMA and

Table 1
The actual composition of the key samples and the phases present.

Sample No.	Actual composition identified by ICP (at.%)			Phases identification		Composition of IM1 identified by EPMA		
	Ca	Mg	Zn	By EPMA	By XRD	Ca	Mg	Zn
1	18.8	74.1	7.1	Mg Mg_2Ca IM1	Mg Mg_2Ca IM1	16.7	66.9	16.4
2	22.4	59.3	18.3	Mg_2Ca IM1	Mg_2Ca IM1	16.7	56.1	27.2
3	18.4	48.8	32.8	Mg_2Ca IM1	Mg_2Ca IM1	16.7	47.8	35.5
4	18.0	44.2	37.8	Mg_2Ca IM1	Mg_2Ca IM1	16.7	43.3	40.0
5	18.0	42.9	40.3	Mg_2Ca IM1	Mg_2Ca IM1	16.7	42.1	41.2
6	15.0	23.1	61.9	IM1 $Ca_2Mg_5Zn_{13}$ IM2*	IM1	16.7	25.4	57.9

IM2* is a new ternary compound, named intermetallic 2 (IM2) in this paper.

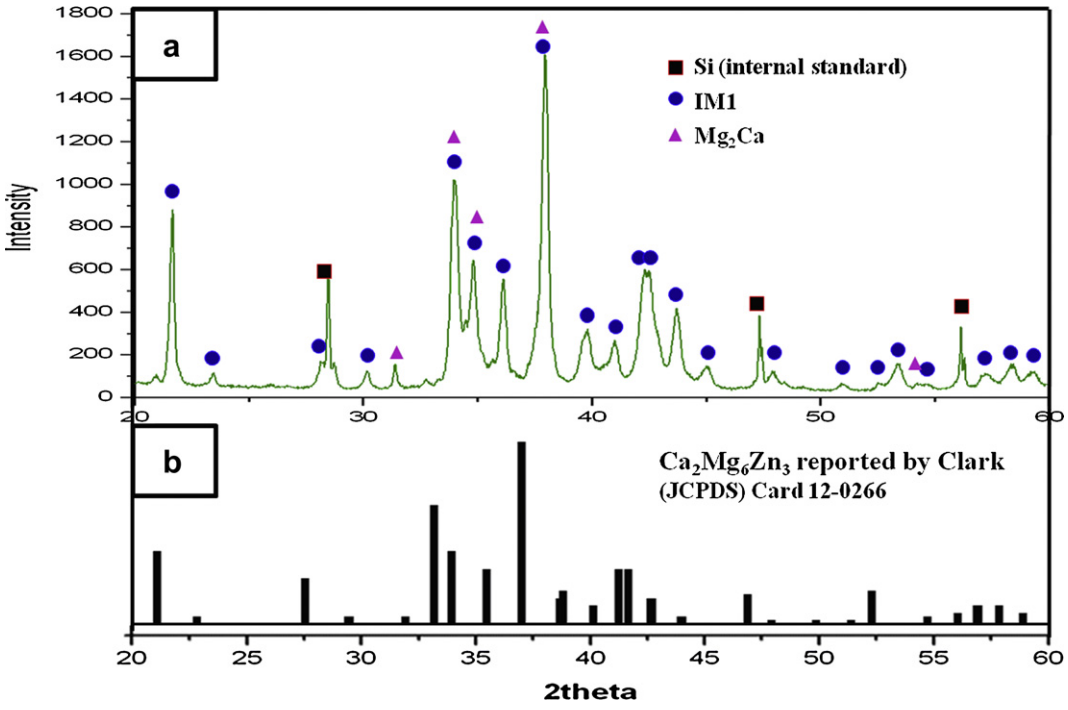

Fig. 5. (a) XRD patterns of key samples 2; (b) XRD pattern reported by Clark [8].

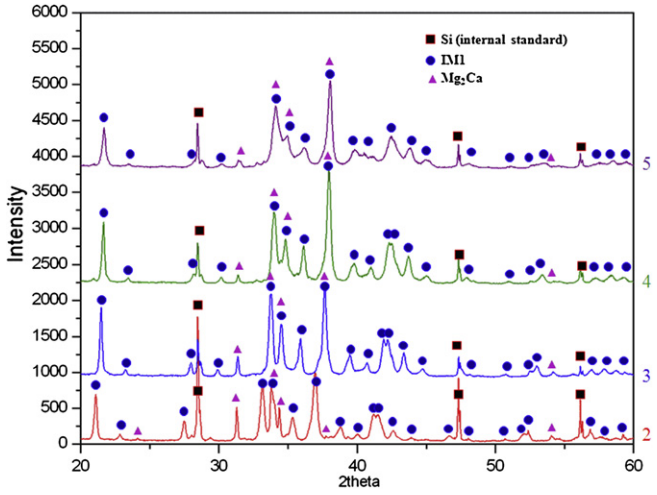

Fig. 6. XRD patterns of the ternary compound IM1 showing the solid solubility effect.

found different from the $Ca_2Mg_6Zn_3$ composition reported in the literature [7,8,10–13]. Hence it has been represented as intermetallic 1 (IM1) in this paper. The result of the EPMA 120 μm line scan of the diffusion couple is shown in Fig. 4. Two phases were identified: $Ca_2Mg_5Zn_{13}$, and IM1 solid solution. The line scan clearly demonstrates that the IM1 compound form substitutional solid solution where Mg substitutes Zn atoms while Ca content remains constant at 16.7 at.%. The least squares approximation was used to establish the concentration profiles of this compound. The change of Mg and Zn concentration profiles show that the substitution of Zn by Mg has a linear relationship with the diffusion distance. The deviation from the linearity is ±2 at.% which is within the error limits of the EPMA measurement. The least squares approximation of the Ca profile shows no changes in its concentration. Based on this diffusion couple, the minimum and maximum solid solubility limits of the IM1 ternary compound determined by EPMA are 35.31 at.% Mg and 65.20 at.% Mg, respectively. Taking into account that the diffusion layers contacting IM1 compound in the diffusion couple do not correspond to the three phase field, it is possible that IM1 compound did not established the maximum

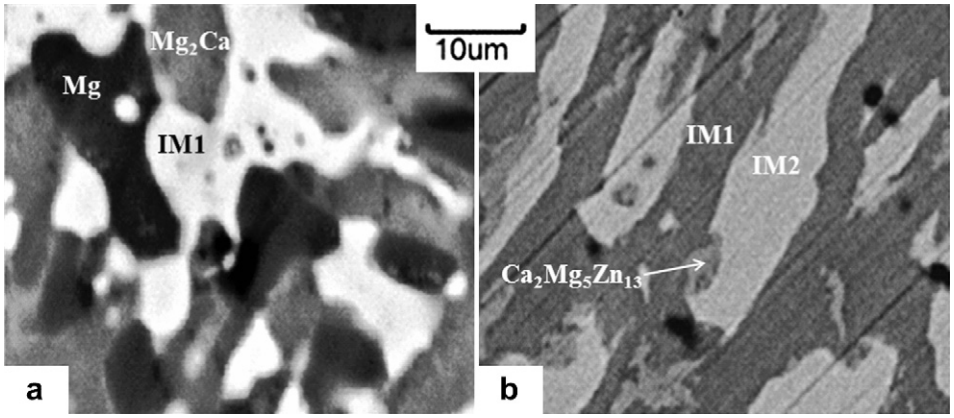

Fig. 7. BE images: (a) sample 1, (b) sample 6. Both are annealed at 335 °C for 4 weeks.

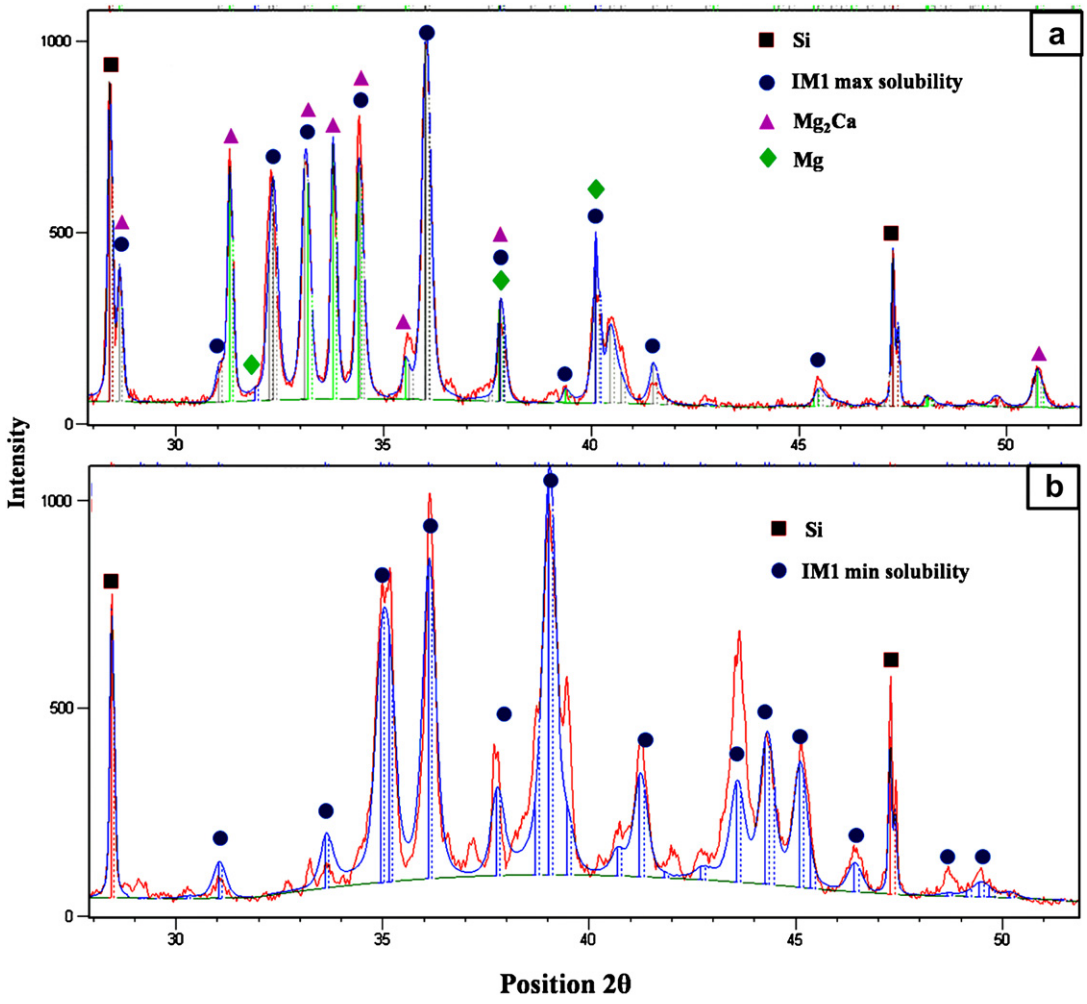

Fig. 8. Rietveld analysis: (a) sample 1, (b) sample 6. Both are annealed at 335 °C for 4 weeks.

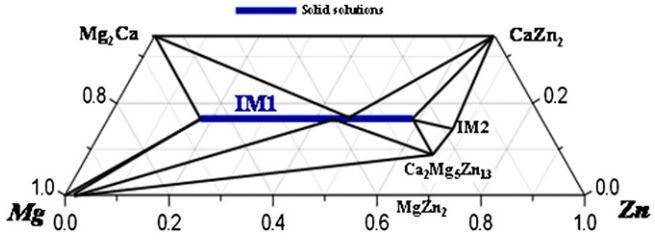

Fig. 9. Partial isothermal section of the Ca–Mg–Zn system at 335 °C showing the phase relations of IM1.

solubility range [16,17]. Therefore, key samples are used to obtain the actual boundaries of this solubility range.

3.2. Key samples analysis

The composition and phase identification of six key samples are summarized in Table 1. The actual chemical compositions of the alloys are measured by ICP and the composition of IM1 compound is determined by EPMA. The phase relations obtained from EPMA show great consistency with the results obtained by XRD. The XRD patterns of key samples 4 annealed at 335 °C for 4 weeks are shown in Fig. 5(a). Full pattern refinement has been carried out by the

Table 2
The chemical composition and unit cell parameters of the IM1 compound determined by EPMA and Rietveld analysis.

Sample No.	Composition of IM1 compound identified by EPMA			IM1 phase composition identified by Rietveld analysis			hexagonal crystal structure, space group $P6_3/mmc$(194) and prototype $Sc_3Ni_{11}Si_4$		
	Ca	Mg	Zn	Ca	Mg	Zn	Unit cell parameters and lattice volume		
							a(Å)	c(Å)	V(Å3)
1	16.7	66.9	16.4	16.7	66.6	16.7	9.958	10.395	892.710
2	16.7	56.1	27.2	16.7	54.5	28.4	9.734	10.169	834.319
3	16.7	47.8	35.5	16.7	46.2	37.1	9.558	10.013	792.139
4	16.7	43.3	40.0	16.7	43.4	39.9	9.486	9.950	775.369
5	16.7	42.1	41.2	16.7	41.9	41.4	9.464	9.925	769.913
6	16.7	25.4	57.9	16.7	25.4	57.9	9.225	9.522	701.803
Paris's [6] data (metallography)	16.7	41.6	41.6	–			–		
Clark's [8] data (XRD)	–			18.2	54.5	27.3[a]	9.725	10.148	831.17
Jardim's [11] data (TEM/EDS)	18.2	54.5	27.3[a]	–			9.7	10	814.84

[a] Recalculated from the $Ca_2Mg_6Zn_3$ formula.

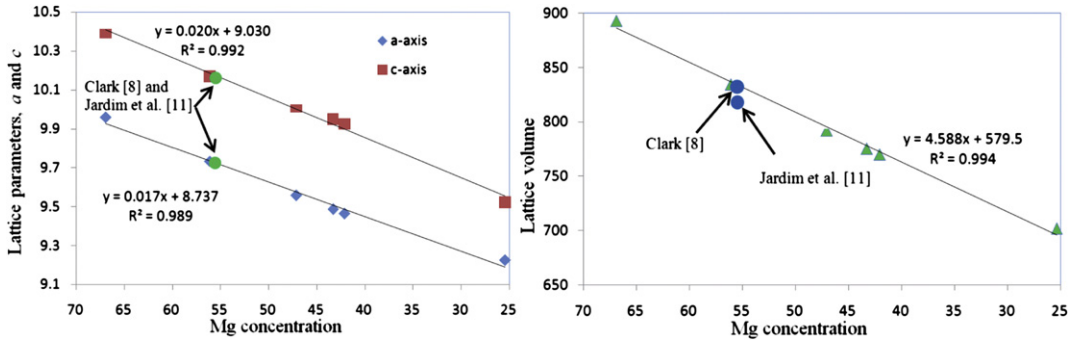

Fig. 10. Cell parameters with Mg concentration for the IM1 compound, where progressive substitution of Mg by Zn decreases the unit cell parameters *a* and *c* and the lattice volume.

Rietveld method. The use of Si as an internal calibration standard enabled correcting the zero shift and specimen surface displacement which are the most serious systematic errors in x-ray powder diffraction patterns. The XRD pattern of sample 4 shows good consistency with that reported by Clark [8] as shown in Fig. 5. The peak positions shift to higher angle with decreasing Mg content. The substitution of Mg by Zn, which has a smaller atomic radius, decreases the unit cell parameters. This is confirmed by the increase of the 2θ values of the peak positions from sample 2–5 due to increasing Zn concentration, as demonstrated in Fig. 6. Combining Pearson's crystallographic database [18] with the Rietveld analysis, IM1 compound is found to have $Sc_3Ni_{11}Si_4$ prototype with hexagonal structure and *P6₃/mmc* (194) space group. The XRD pattern generated using $Sc_3Ni_{11}Si_4$ prototype perfectly corresponds to the experimental patterns reported by Clark [8] and Larinova et al. [10]. However, this crystal structure contradicts with the trigonal structure reported by Jardim et al. [11] and Oh-ishia et al. [13]. Also the XRD pattern generated using $Si_2Te_6Mn_3$ prototype does not match with the current experimental results.

In order to determine the phase boundaries of IM1 ternary compound, two ternary samples 1 and 6 have been prepared to identify the maximum and minimum solid solubility. Backscattered electron images of these samples are presented in Fig. 7. Sample 1 contains three phases: (IM1), (Mg) and Mg_2Ca. The maximum solid solubility of IM1 has been determined by EPMA as 66.9 at.% Mg. The XRD pattern is illustrated in Fig. 8(a). It demonstrates the Rietveld analysis for the IM1, Mg_2Ca and Mg phases in sample 1. Sample 6 contains three phases, the dominating phase is IM1. The minimum solid solubility of IM1 has been determined by EPMA as 25.4 at.% Mg. The XRD pattern is illustrated in Fig. 8(b). $Ca_2Mg_5Zn_{13}$ is not detected in the XRD pattern due to its small relative amount.

Combining the EPMA results of the solid–solid diffusion couple and key alloys, the actual composition of the Mg-rich ternary compound and its complete homogeneity range have been determined. Taking into account the structure type of IM1, the formula of this compound is $Ca_3Mg_xZn_{15-x}$ ($4.6 \leq x \leq 12$) at 335 °C. Partial isothermal section of the Ca–Mg–Zn system at 335 °C and the phase relations are illustrated in Fig. 9. The actual chemical composition of this ternary compound has been measured quantitatively by EPMA/WDS, which shows great consistency with the

Table 3
Refined crystal structure parameters of the IM1 solution compound.

Samples No.	Atomic coordinates (Wyckoff Position)	Occupancy (%)	Reliability factors[a]		
			R_e	R_{wp}	*s*
1	Ca-6h	Ca 100.0	12.1	15.8	1.71
	Zn1-6g	Zn 99.9			
	Mg1-6h	Mg 100.0			
	Mg2-12k	Mg 100.0			
	Mg3-4f	Mg 100.0			
	Mg4-2b	Mg 100.0			
2	Ca-6h	Ca 100.0	11.2	16.9	2.27
	Zn1-6g	Zn 99.8			
	Mg,Zn1-6h	Mg 26.9			
	Mg2-12k	Mg 100.0			
	Mg3-4f	Mg 100.0			
	Mg4-2b	Mg 100.0			
3	Ca-6h	Ca 99.9	11.0	20.5	3.44
	Zn1-6g	Zn 100.0			
	Zn2-6h	Zn 100.0			
	Mg,Zn2-12k	Mg 97.7			
	Mg,Zn3-4f	Mg 80.8			
	Mg,Zn4-2b	Mg 82.2			
4	Ca-6h	Ca 100.0	10.4	20.5	3.87
	Zn1-6g	Zn 100.0			
	Zn2-6h	Zn 99.8			
	Mg,Zn2-12k	Mg 94.8			
	Mg,Zn3-4f	Mg 71.1			
	Mg,Zn4-2b	Mg 82.2			
5	Ca-6h	Ca 100.0	10.3	19.6	3.61
	Zn1-6g	Zn 100.0			
	Zn2-6h	Zn 100.0			
	Mg,Zn2-12k	Mg 93.3			
	Mg,Zn3-4f	Mg 66.2			
	Mg,Zn4-2b	Mg 64.5			
6	Ca-6h	Ca 100.0	10.9	22.3	4.18
	Zn1-6g	Zn 99.8			
	Zn2-6h	Zn 100.0			
	Mg,Zn2-12k	Mg 59.5			
	Mg,Zn3-4f	Mg 31.3			
	Mg,Zn4-2b	Mg 40.7			

[a] Reliability factors: *s* presents the goodness of fit; R_{wp} is the weighted summation of residuals of the least squared fit; R_e is the value statistically expected.

Table 4
Atomic bond lengths of the IM1 compound in sample 1. The bold values represent the shortest atomic bond.

Atom1	Atom2	Distance (Å)
Mg2	Ca	3.5291
Mg2	Ca	3.5234
Mg2	Mg2	3.3052
Mg2	Mg2	3.4156
Mg2	Mg1	**3.1014**
Mg2	Mg3	3.1234
Mg2	Mg4	3.2660
Ca	Mg3	3.4984
Ca	Mg4	3.3117
Ca	Ca	4.2224
Ca	Mg1	3.4446
Ca	Zn1	3.7352
Mg2	Zn1	3.0540
Mg1	Zn1	**2.8088**
Mg3	Zn1	2.8761
Mg1	Mg1	3.1329
Mg1	Mg3	3.2399

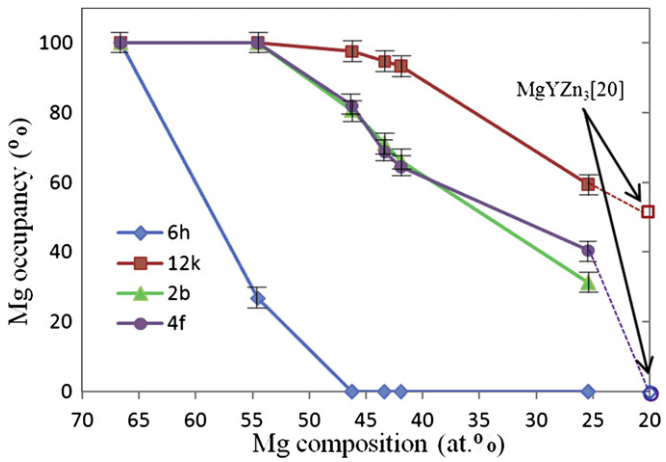

Fig. 11. Mg occupancy in the lM1 compound as a function of Mg concentration.

results obtained by Rietveld approach, as summarized in Table 2. Furthermore, refinement of the XRD patterns was carried out by Rietveld analysis. All XRD data has shown that this solid solution, in six samples, crystallizes in hexagonal structure with *P63/mmc* (194) space group and $Sc_3Ni_{11}Si_4$ prototype. Fig. 10 shows the cell parameters variations with Mg concentration, where substitution of Mg by Zn decreases the unit cell parameters *a* and *c* (Å), and the lattice volume (Å^3). This is shown in more details in Table 2. The linear relation between the lattice parameters, lattice volume and Mg concentration obeys Vegard's law [19] indicating clearly the occurrence of substitutional solid solubility. The composition $Ca_2Mg_6Zn_3$ reported by Clark [8] and Jardim et al. [11] is very close to sample 2, and they reported consistent unit cell parameters with the current work, as can be observed in Table 2 and Fig. 10.

Table 3 shows the refined structural parameters of the IM1 compound and the reliability factors. The decrease in all unit cell parameters is in favor of the occupation of 6h sites by Zn from sample 1 to sample 2. The prerequisite substitutional position of 6h sites has also been confirmed by the shortest bond lengths of Mg1−x (x = Ca, Zn, Mg1, Mg2, Mg3) in sample 1, as can be seen in Table 4. Most of the bond lengths with Mg1 (6h atomic coordinates) demonstrate relatively short distance, indicating that the Mg1 position has higher potential to be substituted by Zn because of the smaller size of Zn atom. For instance, the bond length of Mg2-Mg1 is 3.1014 Å, and the distance between Mg2-Mg2, Mg2-Mg3 and Mg2-Mg4 is 3.4156 Å, 3.1234 Å and 3.2660 Å, respectively. It is obvious that the bond length of Mg2-Mg1 shows the shortest distance, suggesting that the Mg1 atomic position is in favor of the substitution of magnesium by Zinc. Once the 6h sites are occupied completely by Zn atoms, as in the fictitious $Ca_2Mg_6Zn_4$ compound, Mg atoms start to be replaced in 4f, 2b and 12k sites by Zn simultaneously. The fractional atomic occupancy of 6h, 4f, 2b and 12k sites of IM1 have been determined as a function of the Mg

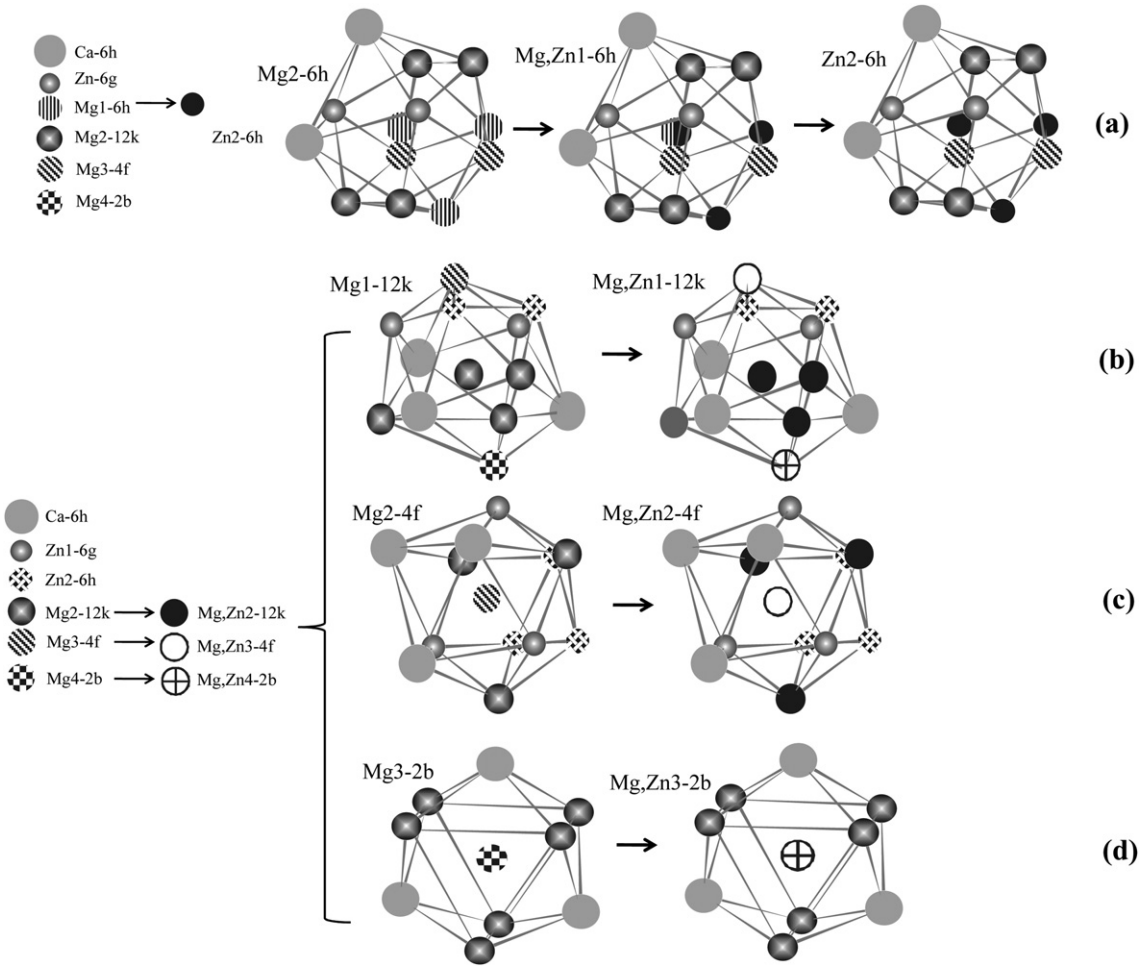

Fig. 12. The coordination spheres of dynamic atomic substitution of magnesium by zinc with different atomic coordinates: (a) substitution of Mg atoms by Zn atoms on 6h sites until they are completely occupied by Zn atoms; (b) to (d) the simultaneous substitution of Mg atoms by Zn atoms on the 12k, 4f and 2b atomic sites.

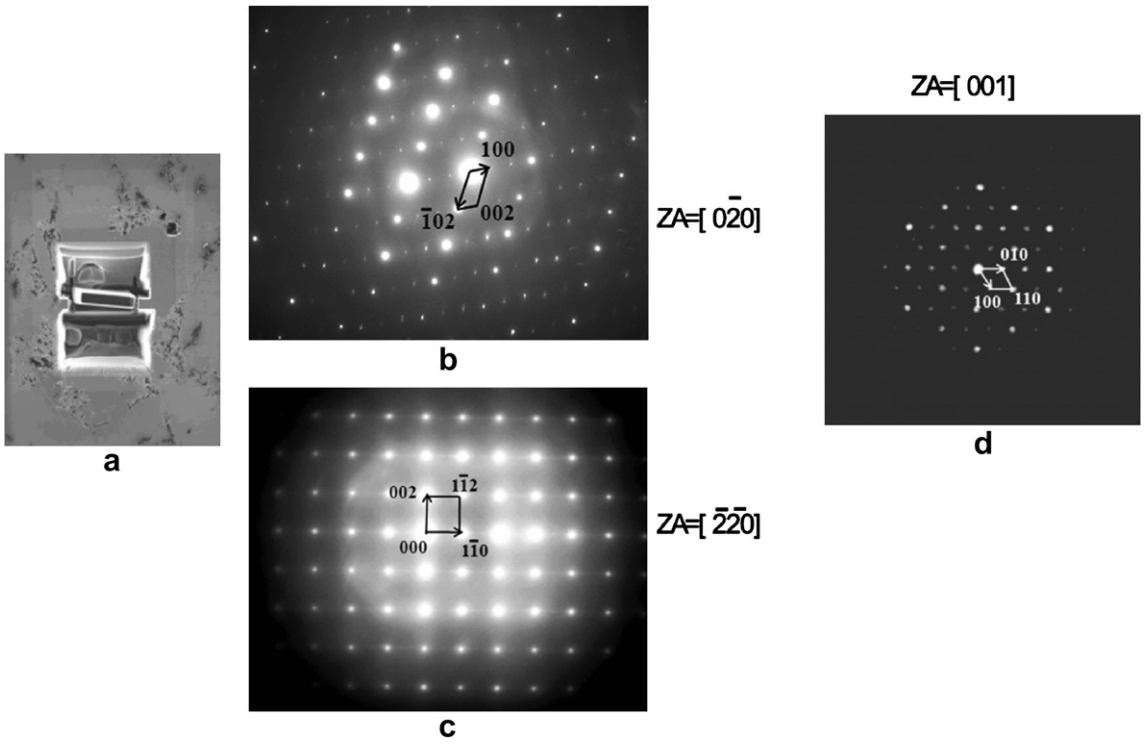

Fig. 13. (a) Using FIB to lift a specimen of the ternary compound; (b) SAED pattern of the sample 4 [0$\bar{2}$0] zone axis indexed as a hexagonal structure; (c) SAED pattern of the sample 4 [$\bar{2}\bar{2}$0] zone axis indexed as a hexagonal structure; (d) SAED pattern of $Ca_2Mg_6Zn_3$ [001] zone axis reported by Jardim et al. [11].

concentration, as shown in Fig. 11. Crystallographic and the site occupancy data of $MgYZn_3$ [20] are similar to IM1 solid solution. The occupancy of 6h, 4f and 12k sites show good consistency with the current experimental results obtained by Rietveld analysis. The occupancy of 2b site has not been used in this comparison, because it involves the mixing of both Y and Mg atoms, whereas in the current case, this site is occupied by Mg and Zn atoms (Y atom is analogous to Ca not to Zn atom).

The coordination spheres and atomic substitution of Mg by Zn for the different atomic coordinates have been identified, as can be seen in Fig. 12. The atomic environment types of 6h, 4f and 12k are deformed icosahedrons as well as 2b sites have a tricapped trigonal prism atomic environment type with the additional three Ca atoms on the sides of the prisms.

3.3. Crystallographic information obtained by TEM

The structure of IM1 single phase region has been studied by TEM. Focused Ion Beam (FIB) was used to lift a specimen of the ternary compound from sample 4 ($Ca_{18.0}Mg_{44.2}Zn_{37.8}$), as shown in Fig. 13(a). According to the crystallographic data obtained by XRD, the hexagonal structure has been indexed and confirmed by means of Selected Area Electron Diffraction (SAED) data, as shown in Fig. 13(b) and (c). The planar spacing, *d* values, obtained from the SAED pattern of sample 4 shows good consistency with the XRD results, as can be seen in Table 5. Furthermore, because of the difference in solid solubility between samples 4 and 2, *d* values determined from sample 2 are slightly larger than those from sample 4 corresponding to the higher content of the larger Mg atom in sample 2. Even though Jardim et al. [11] reported different structure type, the *d* values calculated from the SAED pattern can be used to compare with the values obtained by XRD from sample 2, since sample 2 and $Ca_2Mg_6Zn_3$ have the sample IM1 compound composition, as shown in Fig. 13(d). It is clearly shown that both series of *d* values obtained from XRD pattern reported by Clark [8] and SAED pattern reported by Jardim et al. [11] show good consistency with the values determined by XRD from sample 2, as detailed in Table 5. In addition, the consistent results of *d* and (hkl)

Table 5
Comparison of planar space (*d* value (hkl)) of the IM1 compound in samples 2 and 4.

(hkl)	*d* (Å) (sample 4)		*d* (Å) (sample 2)		
	By XRD (in this work)	From SAEDP (in this work)	By XRD (in this work)	From JCPDS card (Clark [8])	From SAEDP (Jardim et al. [11])
100	8.211	8.223	8.440	8.400	8.4
002	4.975	4.958	5.064	5.100	5.0
110	4.743	4.760	4.867	4.900	4.85
102	4.251	4.275	4.351	–	4.36
112	3.430	3.460	3.514	–	–
300	2.731	2.724	2.809	2.800	–
004	2.486	2.479	2.527	2.530	–
220	2.370	2.380	2.433	2.430	–
114	2.202	2.223	2.253	2.250	–
222	2.140	2.148	2.194	2.190	–
224	1.723	1.728	1.757	1.752	–

values obtained from XRD and SAED patterns support the fact that this ternary compound has the said hexagonal structure.

Moreover, modeling of the intermetallic solid solution requires information regarding the crystal structure of the phases and their homogeneity ranges. From the crystallographic data obtained in this work, the following sublattice model is applied to represent the current compound:

$(Ca)_6(Zn)_6(Mg,Zn)_6(Mg,Zn)_{12}(Mg,Zn)_4(Mg,Zn)_2$ – *Model I.*

Considering the atomic positions and site occupancy from the current experimental results, the atomic occupancy of 4f and 2b demonstrate the same tendency, as shown in Fig. 11. Thus, these two sites should be coupled to reduce the number of end members. The sublattice model can be modified to:

$(Ca)_6(Zn)_6(Mg,Zn)_6(Mg,Zn)_{12}(Mg,Zn)_6$ – *Model II.*

Model II can be simplified further in order to have a more practical sublattice model suitable for thermodynamic modeling of this compound. This can be achieved using the similarity in the coordination numbers and the site occupancy information obtained in this work. The final model for this compound can be written as:

$(Ca)(Zn)(Mg,Zn)_4$ – *Model III.*

This model provides a solubility range of $0 \leq Mg \leq 66.7$ at.% and $16.7 \leq Zn \leq 83.3$ at.%, which covers the wide homogeneity range of the $Ca_3Mg_xZn_{15-x}$ ($4.6 \leq x \leq 12$ at 335 °C) compound.

4. Conclusions

The composition and homogeneity range of the Mg-rich ternary compound in the Ca–Mg–Zn system have been determined. The formula of this compound is $Ca_3Mg_xZn_{15-x}$ ($4.6 \leq x \leq 12$) at 335 °C. It has hexagonal structure with P63/*mmc* (194) space group and $Sc_3Ni_{11}Si_4$ prototype. The lattice parameters increase linearly with increasing Mg content obeying Vegard's law. The site occupancy of 6h, 4f, 2b and 12k has been presented as a function of Mg concentration. Selected area electron diffraction data and the planar spacing *d* values obtained by Rietveld analysis demonstrate excellent consistency. Combining the atomic occupancy results and the crystallographic details obtained in this work, a three sublattice $(Ca)(Zn)(Mg,Zn)_4$ model is suggested for this compound.

Acknowledgments

Financial support from General Motors of Canada Ltd. and NSERC through the CRD grant program is gratefully acknowledged. The authors would like to acknowledge Jean-Marc Joubert for the useful discussion and suggestions at the CALPHAD XXXIX conference in 2010. The help of Ming Wei and Alain Tessier of the Chemistry Department of Concordia University in conducting the ICP measurement is appreciated.

References

[1] Luo AA. Recent magnesium alloys development for elevated temperature application. International Materials Review 2004;49(1):13–30.
[2] Aljarrah M, Medraj M, Wang X, Essadiqi E, Dénès G, Muntasar A. Experimental Investigation of the Mg-Al-Ca system. Journal of Alloys and Compounds 2007;438(1–2):131–41.
[3] Nie F, Muddle BC. Precipitation hardening of Mg-Ca (-Zn) alloys. Scripta Materialia 1997;37(34):1475–81.
[4] Zberg B, Uggowitzer PJ, Löffler JF. MgZnCa glasses without clinically observable hydrogen evolution for biodegradable implants. Nature Materials; 27th Sep. 2009. Published Online.
[5] Zberg B, Arataa ER, Uggowitzera PJ, Löffler JF. Tensile properties of glassy MgZnCa wires and reliability analysis using weibull statistics. Acta Materialia 2009;57(11):3223–31.
[6] Paris R. Ternary Alloys, Publications Scientifiques et Techniques du Ministère de L'Air. Ministère de L'Air 1934;(45):1–86.
[7] Clark JB. The solid Constitution in the Mg-rich region of the Mg–Ca–Zn phase diagram. Transactions of the Metallurgical Society of AIME 1961;Vol. 221:644–5.
[8] Clark JB. Joint Committee on Powder Diffraction Standards (JCPDS) Card 12-0266; 1961.
[9] Clark JB. Joint Committee on Powder Diffraction Standards (JCPDS) Card 12-0569; 1961.
[10] Larinova TV, Park WW, You BS. A ternary phase observed in rapid solidified Mg–Ca–Zn alloys. Scripta Materialia 2001;45:7–12.
[11] Jardim PM, Solorzano G, Sande JBV. Precipitate crystal structure determination in melt spun Mg-1.5wt%Ca-6wt%Zn Alloy. Mircoscopy and Microanaysis 2002;8:487–96.
[12] Jardim PM, Solorzano G, Sande JBV. Second phase formation in melt-spun Mg–Ca–Zn alloys. Materials Science and Engineering A 2004;381(1–2):196–205.
[13] Oh-ishia K, Watanabe R, Mendis CL, Hono K. Age hardening response of Mg-0.3 at.% Ca alloys with different Zn contents. Materials Science and Engineering A 2009;526(1–2):177–84.
[14] Wasiur-Rahman S, Medraj M. Critical assessment and thermodynamic modeling of the binary Mg–Zn, Ca–Zn and ternary Mg–Ca–Zn systems. Intermetallics 2009;17(10):847–64.
[15] Kotur BY, Sikiritsa M, Bodak OI, Gladyshevskii EI. Crystal structure of the compound Sc3Ni11Si4. Soviet Physics Crystallography 1983;28:387–9.
[16] Kirkaldy JS, Brown LC. Diffusion behavior in the ternary multiphase systems. Canadian Metallurgical Quarterly 1963;2(1):90–115.
[17] Kodentsov AA, Bastin GF, Van Loo FJJ. The diffusion couple technique in phase diagram determination. Journal of Alloys and Compounds 2001;320(2):207–17.
[18] Holger Putz. Klaus Brandenburg, Pearson's crystal data, crystal structure database for inorganic compounds, CD-ROM software version 1.3.
[19] Denton AR, Ashcroft NW. Vegard's Law. The American Physical Society 1991;43(6):3161–4.
[20] Deng DW, Kuo KH, Luo ZP, Miller DJ, Kramer MJ, Dennis KW. Crystal structure of the hexagonal Zn_3MgY phase. Journal of Alloys and Compounds 2004;373(1–2):156–60.